Available online at www.sciencedirect.com

SciVerse ScienceDirect

Ceramics International 38 (2012) 6599–6605

CERAMICS INTERNATIONAL

www.elsevier.com/locate/ceramint

Erosion behavior of B_4C based ceramic nozzles by abrasive air-jet

Sun Junlong[a], Liu Changxia[a,*], Tian Jin[b], Feng Baofu[a]

[a]*Key Laboratory of Advanced Manufacturing and Automation Technology, Ludong University, Yantai 264025, Shandong Province, PR China*
[b]*Quzhou College, Quzhou 324000, Zhejiang Province, PR China*

Received 7 December 2011; received in revised form 9 May 2012; accepted 17 May 2012
Available online 7 June 2012

Abstract

TiC and Mo were introduced into B_4C-based ceramic nozzles, which were obtained by hot-press sintering. The effect of TiC content on mechanical properties and erosion behavior of B_4C-based ceramic nozzles were analyzed. XRD analysis showed that chemical reactions took place during the sintering process, which resulted in $B_4C/Mo/TiB_2$ ceramic nozzle with high density and improved mechanical properties compared with B_4C/Mo ceramic nozzle. The sintering temperature was decreased from 2150 °C for B_4C/Mo ceramic nozzle to 1950 °C for $B_4C/Mo/TiB_2$ ceramic nozzle. Results of erosion wear tests indicated that the hardness and toughness were the key factors influencing the erosion rate of $B_4C/Mo/TiB_2$ ceramic nozzle. Analysis of the eroded bore surfaces of $B_4C/Mo/TiB_2$ ceramic nozzle showed that the entry bore section exhibited a brittle fracture induced material removal process, and the center bore section showed plowing and polishing of material removal. Fracture and plowing of material removal occurred at the exit bore section.

Keywords: Erosion behavior; B_4C; Mo; Ceramic nozzle

1. Introduction

Sandblast is widely applied in the field of mechanical engineering, chemical industry, etc. Nozzle is one of the key components affecting the sandblast process. B_4C has an excellent hardness, a high melting point, low specific weight and good chemical inertness at room temperature [1,2]. Especially, B_4C is best recognized for its high hardness and erosion resistance, making it a promising candidate for wear resistance component. Abrasive air-jet nozzles made of boron carbide with high relative density and excellent wear resistance provides a longer life compared with those made of other materials [3,4]. However, it is difficult to sinter pure B_4C close to theoretical density due to the low diffusion of B_4C. Researchers have attempted to accelerate the sintering process of B_4C and improve its mechanical properties by incorporating second phases such as TiB_2, (W,Ti)C, SiC and Al_2O_3/TiB_2 into B_4C, and many interesting results have been obtained [4–6].

There commonly exists in commercial B_4C powder a few impurities (B_2O_3), forming a compact layer in the sintering process and restraining the sintering of B_4C-based ceramics. Carbon is regarded as an effective additive to accelerate the densification of B_4C by eliminating the detrimental role of B_2O_3. The addition of carbon in B_4C ceramic, however, decreases its mechanical properties. Hence we try to find an approach to eliminate B_2O_3 without the addition of carbon in our studies.

Although there are considerable interests on the erosion of ceramic materials, little work has been reported on the erosion behavior of $B_4C/Mo/TiB_2$ ceramic nozzles. In this paper, $B_4C/Mo/TiB_2$ ceramic nozzles with different contents of TiC were prepared by hot-pressing. TiC was expected to eliminate B_2O_3 and accelerate the densification of B_4C based ceramic nozzles. The mechanical properties and microstructures of the nozzles were investigated. Furthermore, erosion experiments were carried out for testing the erosion behavior of $B_4C/Mo/TiC$ ceramic nozzles.

2. Experimental procedure

The grain sizes of B_4C, Mo and TiC were 3–5 μm, 0.5 μm and 3 μm, respectively. B_4C/Mo (mass ratio 18:1) was used as the base material. The mixtures of B_4C and Mo were homogenized with ethanol in vibratory ball mill for 60 h

*Corresponding author. Tel.: +86 158 66472136.
E-mail address: hester5371@yahoo.com.cn (L. Changxia).

0272-8842/$36.00
http://dx.doi.org/10.1016/j.ceramint.2012.05.045

Table 1
Starting compositions, mechanical properties, preparation parameters of B_4C/Mo based ceramic nozzles.

Samples	Compositions (wt %)	Hardness (GPa)	Fracture toughness (MPa .$m^{1/2}$)	Bending strength (MPa)	Relative density (%)	Preparation parameters	
						Temperature (°C)	Time ($_{min}$)
SA00	100%(B_4C+Mo)	21.0 ± 1.3	3.3 ± 0.6	450 ± 30	94.6 ± 0.5	2150	60
SA05	95%(B_4C+Mo)+5%TiC	22.5 ± 1.2	4.0 ± 0.5	445 ± 28	96.0 ± 0.3	1950	60
SA10	90%(B_4C+Mo)+10%TiC	24.3 ± 1.1	4.3 ± 0.4	525 ± 36	98.5 ± 0.5	1950	60
SA15	85%(B_4C+Mo)+15%TiC	24.3 ± 1.0	3.2 ± 0.4	530 ± 25	98.6 ± 0.2	1950	60
SA20	80%(B_4C+Mo)+20%TiC	23.1 ± 1.0	3.1 ± 0.5	480 ± 30	98.1 ± 0.3	1950	60

using cemented carbide balls. TiC was added to B_4C/Mo mixtures according to the combinations listed in Table 1 and was ball milled for 60 h to obtain a homogeneous mixture. The container with an internal diameter of 150 mm is made of cemented carbide, rotating with a speed of 100 r/min. The average particle size of the final milled powders was less than 1.5 μm. Then the mixtures were washed in 10% (mol.) hydrochloric acid to remove metal impurities.

Six samples, chosen from one nozzle with the same compositions, were used for measuring the density and mechanical properties at room temperature. Test samples were cut with dimension of 3 mm × 4 mm × 30 mm for measuring mechanical properties. Three-point-bending mode was used to measure the bending strength using an electronic universal experimental instrument with a span of 20 mm at a crosshead speed of 0.5 mm/min (produced by Jinan TEST Co., Ltd.). Vickers hardness was measured on polished surface with a load of 9.8 N for 5 s with a micro-hardness tester (MH-6). Fracture toughness measurement was performed using the indentation method with a hardness tester (Hv-120). The density of samples was determined by the Archimedes method. For hardness and fracture toughness, the average of twelve indentation results for each sample was adopted in order to minimize data scattering and decrease the relative error.

Erosion wear tests were conducted with a GS-6 abrasive air-jet machine, and the schematic diagram of the equipment is shown in Fig. 1. Nozzles were washed by ultrasonic in ethanol for 30 min after erosion, and weight loss was tested by an electronic balance. The compressed air pressure was set at 0.4 MPa. The erodent abrasives were silicon carbide (SiC) powders with grain size of 165–185 μm, hardness of 32.8–34 GPa and density of 3.15 g/cm^3. The phases of the fabricated B_4C based ceramic nozzles were determined using XRD (D/max-2400). Microstructures and eroded surfaces of the fabricated nozzles were examined with a scanning electron microscope (HITACHI S-570).

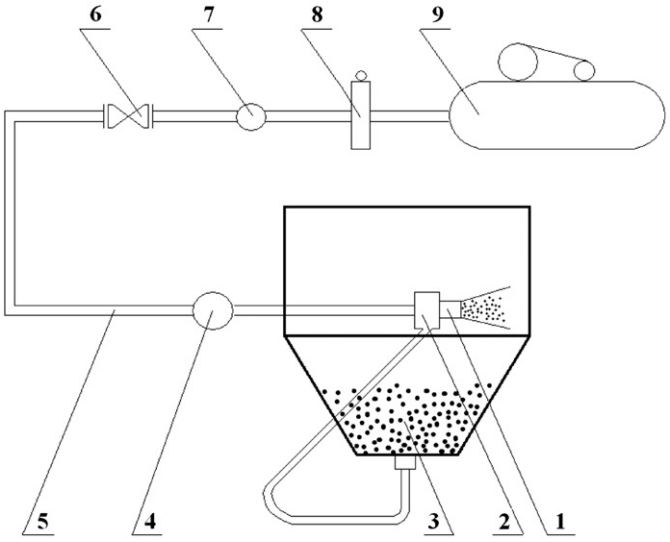

Fig. 1. Schematic diagram of the abrasive air-jet machine tool (1. ceramic nozzle, 2. blasting gun, 3. sand hopper, 4. flow meter, 5. air supply tube, 6. control valve, 7. pressure gage, 8. filter, 9. air compressor).

3. Result and discussion

3.1. X-ray diffraction phase analysis

Fig. 2 shows the XRD analysis of SA10 sample sintered at 1950 °C for 60 min. There were B_4C, TiB_2, Mo phases in the sample and no trace of TiC was found. TiB_2 may be formed by the following reaction:

$$B_4C + 2TiC \rightarrow 2TiB_2 + 3C \quad (1)$$

Based on the thermodynamic analysis of chemical reactions [7,8], the value of the Gibbs free energy (ΔG_T^{θ}) of Eq. (1) was less than zero, which indicated that the equation could occur during the sintering process. Simultaneously, C was produced as shown in Eq. (1), which may contribute to enhance the densification of B_4C based ceramic nozzles, as C can eliminate boron oxide impurity. The following reaction took place during the hot-press sintering process: [9]

$$B_2O_3 + 7C \rightarrow B_4C + 6CO \quad (2)$$

Some C formed as shown in Eq. (1) eliminated boron oxide impurity, accelerating the densification of B_4C based ceramics, and the left C in SA10 sample may be too small to be determined by XRD.

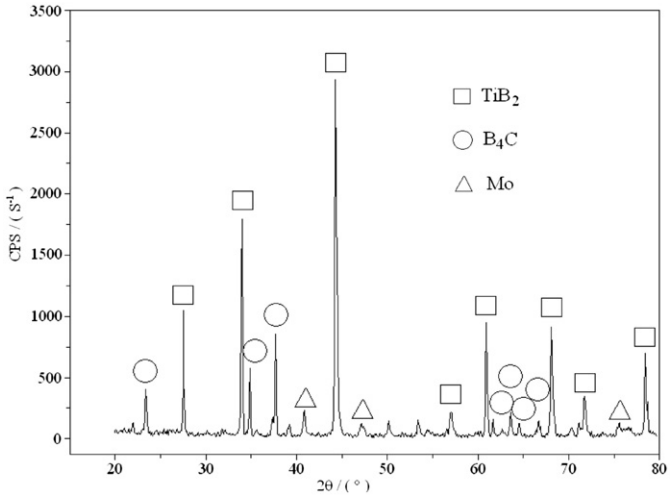

Fig. 2. X-ray diffraction analysis of the SA10 sample.

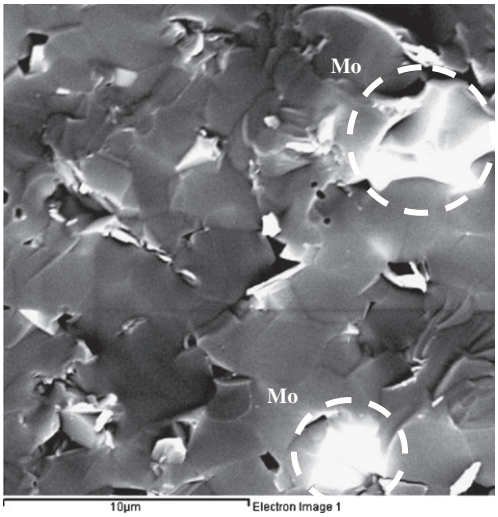

Fig. 3. SEM photograph of fracture surface of SA00 sample.

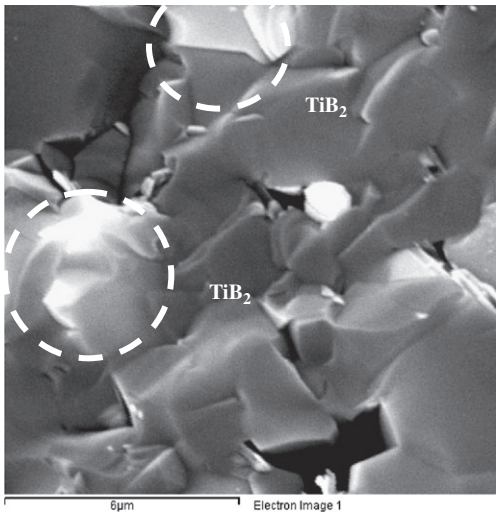

Fig. 4. SEM photograph of fracture surface of SA10 sample.

3.2. Mechanical properties and microstructures of the nozzles

The relative densities and mechanical properties of B_4C based ceramic nozzles are shown in Table 1. The relative densities of all samples with TiC addition sintered at 1950 °C were higher than 95%, while that of the sample without TiC addition sintered at 2150 °C was only 94.6%. The relative density increased with the increase in the TiC content, and the sintering temperature was lowered from 2150 °C for B_4C/Mo ceramic nozzle to 1950 °C for B_4C/Mo/TiC ceramic nozzle. The improved relative density may be mainly due to the elimination of boron oxide impurity and the quantity of heat produced as shown in Eqs. (1) and (2). Being produced by chemical reaction and distributed homogeneously in the nozzle, the in-situ formed TiB_2 had more surface energy than those directly incorporated into B_4C based ceramic nozzles, which could be another reason that contributed to accelerate the sintering of B_4C/Mo/TiC ceramic nozzles.

It could be seen from Table 1 that B_4C/Mo/TiC ceramic nozzles showed better overall performance, with respect to B_4C/Mo ceramic nozzles fabricated at a higher sintering temperature. The hardness raised from 21 GPa to 24.3 MPa as TiC content increased from 0 to 10 wt%. The trend of the bending strength and fracture toughness were similar with that of the hardness. The hardness, fracture toughness and bending strength of SA10 sample reached 24.3 GPa, 4.3 MPa $m^{1/2}$ and 525 MPa respectively, which were enhanced by 15.7%, 30.3% and 16.7%, respectively, with respect to SA00 sample.

SEM photomicrographs of fracture surfaces for SA00 and SA10 sample are shown in Figs. 3 and 4. In Fig. 3, the dark area was identified by EDX analysis to be B_4C and the light area to be Mo. The dark area in Fig. 4 was also B_4C and the light area was TiB_2. The grain shapes were irregular and some porosity appeared in SA00 sample as seen in Fig. 3. These pores served as fracture origins and led to the degradation of strength and fracture toughness. In addition to this, there existed a transgranular cleavage, which could decrease the fracture toughness of SA00 sample. SA10 sample had a more homogeneous microstructure and few pores existed, which may contribute to the improved bending strength and fracture toughness. The fracture mode of SA00 sample was mainly transgranular failure, while the pull-out of grains was observed in SA10 sample, so the fracture mode turned to the combination of transgranular failure and intergranular failure for SA10 sample. Some researchers considered transgranular fracture for B_4C based ceramics denoting low rapture energy and mixed fracture mode meaning high rapture energy [5,10,11]. Therefore, the variation of fracture mode contributed to the enhanced mechanical properties for SA10 sample. Higher relative density, more uniform microstructures, mixed fracture mode associated with the

reduction of porosity may be the main reason contributed to the improved hardness, fracture toughness and bending strength of B_4C/Mo/TiC ceramic nozzles [3,8]

3.3. Erosion behavior of B_4C/Mo/TiC ceramic nozzles

Fig. 5 illustrates the cumulative mass loss of B_4C/Mo/TiC ceramic nozzles in abrasive air-jet. It was noted that the cumulative mass loss continuously increased with the erosion time, and SA10 sample showed the best erosion resistance under the same test conditions. The worn nozzle entry and exit bore diameter variation with the erosion time are shown in Fig. 6. It was shown that for both entry and exit the bore diameter increased linearly with the erosion time and enlarged fast up to 90 min operation, and then it enlarged gradually for the following 150 min of operation, which indicated that the erosion rate in the entry and exit reached a maximum from 0 to 90 min operation. The reason that resulted in this phenomenon may be that erosion rate of B_4C/Mo/TiC ceramics increased with the increase in the impact angle [12]. Within further 150 min operation, the relation between bore diameter variation and the erosion time changed owing to the decreased impact angle. The entry and exit bore section of SA10 sample after 240 min operation is shown in Fig. 7. The entry bore section was severely worn, while the exit bore was slightly worn, indicating that the impact angle in the entry bore was bigger than that in the exit bore section.

The erosion rates of the nozzles are shown in Fig. 8. The values of wear rate were 1.95, 1.422, 0.845, 1.059 and 1.4 for SA00, SA05, SA10, SA15 and SA20 respectively. Erosion rates of samples with in-situ formed TiB_2 were lower than that of sample without TiB_2. Many researches showed that erosion properties of nozzle were significantly affected by their mechanical properties [3,4,6,12]. Therefore

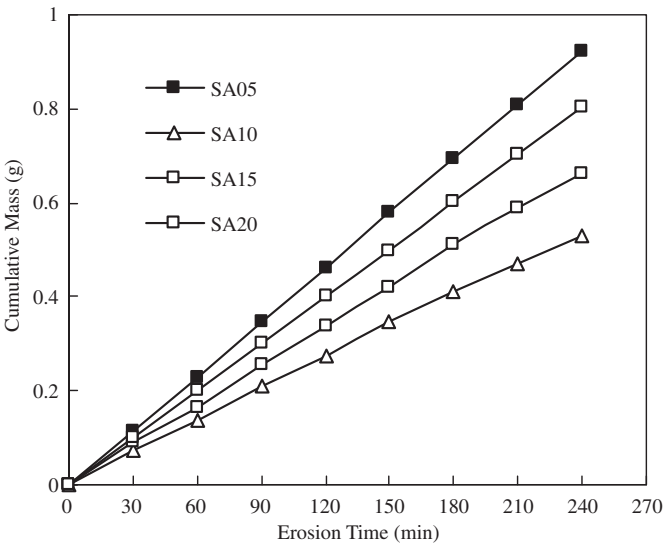

Fig. 5. The cumulative mass loss of B_4C/Mo/TiC ceramic nozzles.

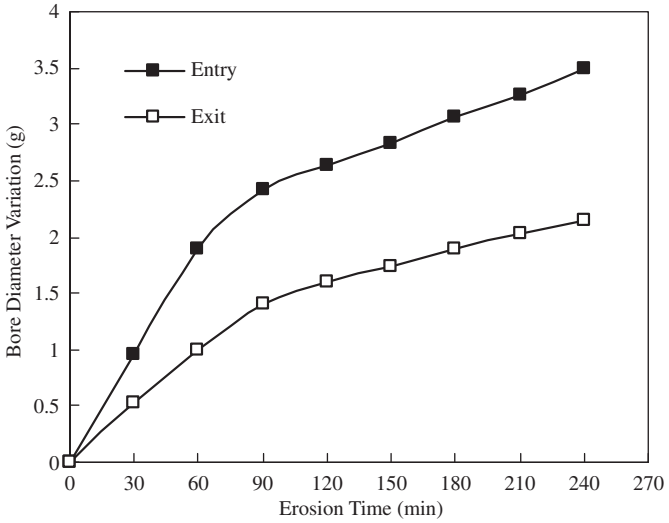

Fig. 6. The entry and exit bore diameter of SA10 sample variation with the erosion time.

the erosion resistance of B_4C/Mo/TiC ceramic nozzles was enhanced may be mainly due to the in-situ formation of TiB_2, which can contribute to the improved mechanical properties of the nozzles.

The following equation can express the relationship between mechanical properties and volume erosion rate E_V [11,13]:

$$E_V \propto \frac{1}{H^{5/2}K_{IC}} \tag{3}$$

where H denotes the hardness, and K_{IC} denotes the fracture toughness. E_V is plotted as a function of the hardness and fracture toughness, as shown in Fig. 9(a). It was seen that E_V increased logarithmically with increase in the reciprocal of product for fracture toughness and 2.5 times hardness. The fracture toughness of SA20 was lower than that of SA05 (Table 1), while the erosion rate of SA05 (with lower hardness) was higher than that of SA20 (with higher hardness), indicating that the hardness of B_4C/Mo/TiC ceramic nozzles influenced their E_v greatly. E_v, decreasing logarithmically with the increasing of hardness, was plotted as a function of hardness in Fig. 9(b). With the same hardness, however, SA10 and SA15 had different erosion rates (Table 1 and Fig. 8), which showed that fracture toughness would play a key role in influencing the erosion behavior of B_4C/Mo/TiC ceramic nozzles with the same hardness.

Fig. 10 shows SEM micrographs of the worn inner bore surfaces of SA10 at different areas after 240 min. There existed differences among the erosion surfaces of entry, middle and exit of B_4C/Mo/TiC ceramic nozzles. A lot of obvious cavities were located on the entry surface, indicating that it suffered from severe impacting, which exhibited the character of fracture induced material removal (Fig. 10(a)). It was relatively smooth at the middle surface by contrast with the entry surface, and some plowing

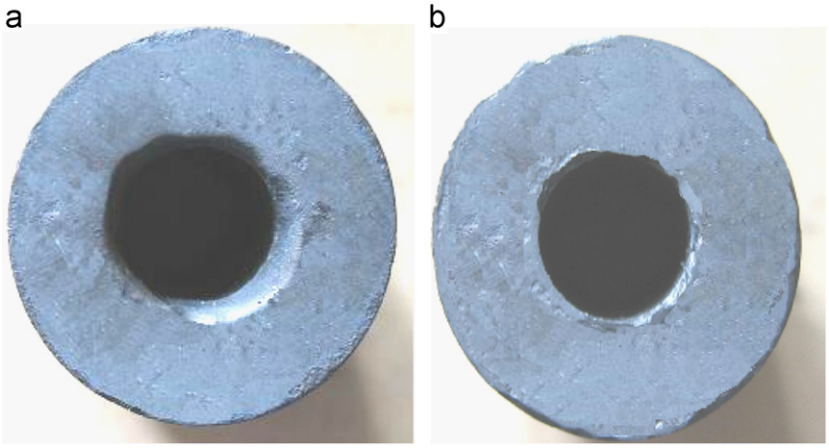

Fig. 7. Bore sections of worn SA10 sample after sand blasting: (a) entry section and (b) exit section.

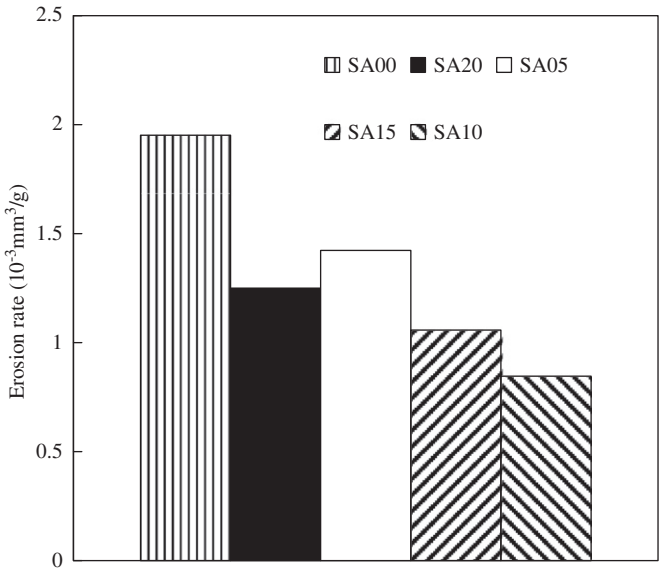

Fig. 8. Erosion rates of B_4C/Mo based ceramic nozzles.

features characteristic could be observed (Fig. 10(b)). The appearance of exit surface showed obvious small pits and scratches, which indicated that material removal of fracture and plowing occurred (Fig. 10(c)).

It is well known that the plastic deformation and the fracture induced material removal are two mechanisms of material removal. The plastic deformation usually appears for ductile material, displaying maximum erosion rate at low impact angles, while the fracture usually appears for brittle material, displaying maximum erosion rate at normal impact angle [14]. Both types of material removal may occur simultaneously for the variation of local stress state, which is influenced significantly by the impact angle. Fig. 11 shows the interaction model of particles with nozzle in sand blasting process. A brittle fracture induced removal in the entry surface may be caused by a large impact angle almost up to 90°. The entry surface suffers from severe abrasive impact, which may cause lateral cracks in the subsurface and facilitates the removal of the material ships [15]. Most of the particles travelled parallel to the nozzle wall at middle section, which indicated that the abrasive particles hit the nozzle at low angles. Erosion at the exit surface was slighter than that at the entry surface, and was severer than that at the middle surface, since the impact angle at the exit surface was smaller than that at the entry surface, and was larger than that at the middle surface. The larger the impact angle was, the severer the erosion would be. It was concluded that the material removal mode of fracture at the entry surface may attribute to the stress at the entry surface almost up to the strength of $B_4C/Mo/TiB_2$ ceramic nozzles, and that of plowing at the middle surface may attribute to the far away lower stress than the strength of the nozzle.

4. Conclusions

$B_4C/Mo/TiC$ ceramic nozzles with different content of TiC were fabricated by hot pressing. The sand erosion performances of $B_4C/Mo/TiC$ ceramic nozzles in abrasive air-jet machining were analyzed. The following conclusions were obtained:

1. Chemical reaction between B_4C and TiC took place and resulted in $B_4C/Mo/TiB_2$ composite with high density and improved mechanical properties compared with B_4C/Mo ceramic nozzle. The sintering temperature was lowered from 2150 °C for B_4C/Mo ceramic nozzle to 1950 °C for $B_4C/Mo/TiB_2$ ceramic nozzle.
2. The hardness of $B_4C/Mo/TiB_2$ ceramic nozzles had an important influence on the erosion rate in sand blasting. The nozzle materials with higher hardness showed lower erosion rate. By having the same hardness, the fracture toughness would play a key role in influencing the erosion behavior of $B_4C/Mo/TiB_2$ ceramic nozzles.

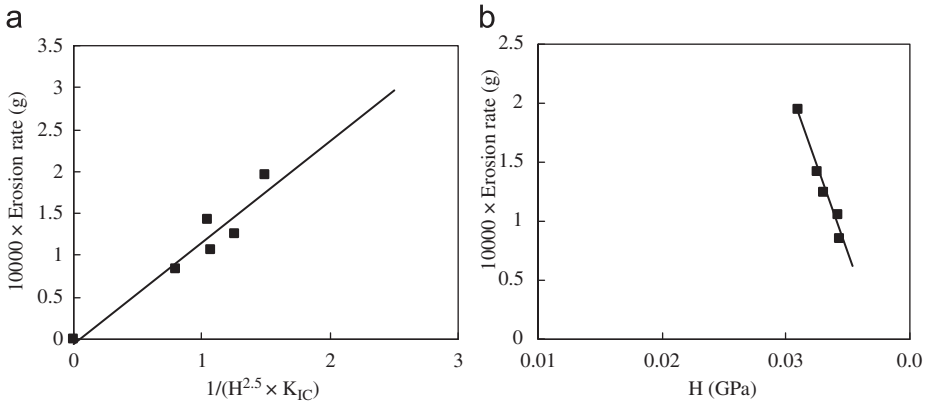

Fig. 9. Effect of $(1/(H^{2.5}K_{IC}))$ and hardness of the erosion rate of B_4C/Mo based ceramic nozzles: (a) $(1/(H^{2.5}K_{IC}))$ and (b) H.

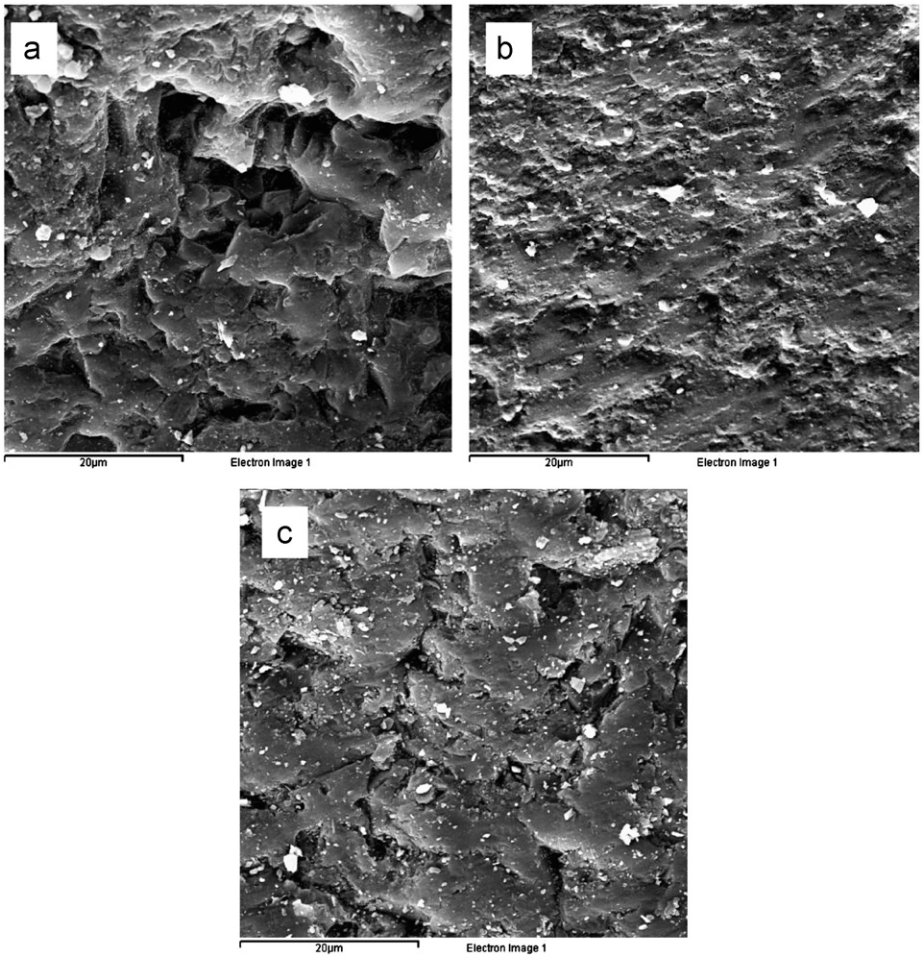

Fig. 10. SEM micrographs of the worn inner bore surfaces of SA10 sample at different areas after 240 min operations: (a) entry, (b) middle and (c) exit surface.

3. Analysis of the eroded bore surfaces showed that the entry bore surface exhibited a brittle fracture induced removal process, while the center bore surface showed plowing and polishing type of material removal mode. Fracture and plowing of material removal model seemed to be occurred at the exit bore surface. The material removal mode of fracture at the entry surface may be attributed to the stress at the entry surface almost up to strength of $B_4C/Mo/TiB_2$ ceramic nozzles, and that of plowing at the middle surface may be due to the far away lower stress than strength of the nozzle.

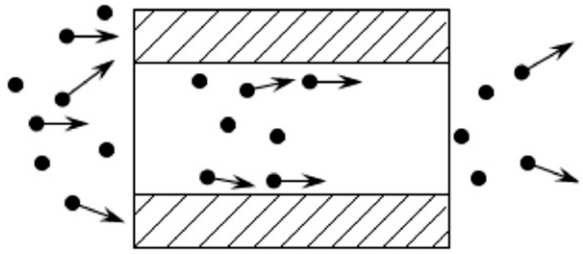

Fig. 11. Interaction of particles with nozzle in sand blasting process.

Acknowledgments

The work described in this paper is supported by the Natural Science Foundation of Shandong Higher Education Institutions of China (no. ZR2011EL026). The Specialized Personnel Invitation Rewards of Ludong University (Nos. LY20074302 and LY20074303).

References

[1] T.K. Roy, C. Subramanian, A.K. Suri, Pressureless sintering of boron carbide, Ceramics International 32 (2006) 227–233.
[2] L. Levin, N. Frage, M.P. Dariel, A novel approach for the preparation of B_4C-based cermets, International Journal of Refractory Metals & Hard Materials 18 (2000) 131–135.
[3] Deng Jianxin, Sun Junlong, Sand erosion performance of B_4C based ceramic nozzles, International Journal of Refractory Metals & Hard Materials 26 (2008) 128–134.
[4] Jianxin Deng, Liu Lili, Ding Mingwei, Sand erosion performance of SiC/(W,Ti)C gradient ceramic nozzles by abrasive air-jets, Design Material sand Design 28 (2007) 2099–2105.
[5] Suzuya Yamada, Giyoshijirao, Yukihiko Yamauchi, huzo Ganzaki, High strength B_4C–TiB_2 composites fabricated by reaction hot-pressing, Journal of the European Ceramic Society 23 (2003) 1123–1130.
[6] Deng Jianxin, Erosion wear of boron carbide ceramic nozzles by a brasive air-jets, Materials Science and Engineering A 408 (2005) 227–233.
[7] D.L. Ye, J.H. Hu, in: Handbook of the Thermodynamic Data of Inorganic Substances, Metallurgical Industry Press, Peking of China, 2002, pp. 57–1061.
[8] Junlong Sun, Changxia Liu, Rugui Wang, Low pressure hot pressing of B_4C matrix ceramic composites improved by Al_2O_3 and TiC additives, Materials Science and Engineering A 518 (2009) 27–31.
[9] L.S. Sigl, Processing and mechanical properties of boron carbide sintered with TiC, Journal of the European Ceramic Society 18 (1998) 1521–1529.
[10] Zhen Yuhua, Li Aiju, Yin Yansheng, Shi Ruixia, Liu Yingcai, Reactive and dense sintering of reinforced-toughened B_4C matrix composites, Materials Research Bulletin 39 (2004) 1615–1625.
[11] K.A. Schwetz, L.S. Sigl, J. Greim, H. Knoch, Wear of boron carbide ceramics by abrasive waterjets, Wear 181–183 (1995) 148–155.
[12] Changxia Liu, Junlong Sun, Erosion behaviour of B_4C-based ceramic composites, Ceramics International 36 (4) (2010) 1297–1302.
[13] B.R. Lawn, A model for crack initiation in elastic/plastic indentation fields, Journal of Materials Science 12 (1977) 2195–2199.
[14] R.F. Cook, B.R. Lawn, A modified indentation toughness technique, Journal of the American Ceramic Society 66 (11) (1983) 200–201.
[15] Jianxin Deng, Xihua Zhang, Pingzhang Niu, et al., Wear of ceramic nozzles by dry sand blasting, Tribology International 39 (2006) 274 R)C28.